Design, Model, and Application of an Electromechanical Variable Stiffness Spring

Mason Mitchell

***Abstract*— This paper outlines a design for a spring that can produce large changes in stiffness in a short period of time, while also maintaining other spring parameters such as relaxed length or diameter. To achieve this, we propose an electromechanically tunable stiffness spring. This mechanism consists of a thin PET sheet bent into a ring with many layers that we can add or remove continuously from the center to change the effective thickness of the ring without affecting its outside diameter. We built a model, and validation using a multitude of practical stiffness tests while changing spring parameters. Finally we demonstrate the capability of our spring in a tunable stiffness manipulator. By using our deformation model, we build a variable stiffness spring segment with 4DOF for millimeter accurate positioning, with rigidity control.**

I. Introduction

Soft robotics is one of the fastest growing research topics in the robotics field [1]. It has major implications in medical robotics, and has provided impactful advances in biological mimicking, dexterous manipulation, and unique locomotion and actuation techniques [2]. With an intrinsic ability to be safe for human-robot interaction, soft robotics is a clear contender for tasks involving human collaboration such as space exploration, or surgery ([3], [4], [5]).

A common device used in constructing these soft robotic structures is a spring. However, classical springs have parameters such as relaxed length, diameter, and stiffness that are fixed and are immutable without causing damage to the structure. Researchers have designed novel springs for their compliant structures that can dynamically change these parameters in order to improve performance and open new avenues of actuation in their device [6]. Typically, the parameter that is altered the most is stiffness. There are many ways to achieve these variable stiffness structures, but we have simplified most of these solutions into two main categories.

Smart materials can be precisely controlled to change their material properties by applying some form of external excitement into the system. One such method uses an electrorheological (ER) fluid, which can vary in viscosity by applying an electric field [7]. There are also electrically actuated polymers that can be excited with an electrical field to stiffen due to compressive electrostatic forces inside the material [8]. Other polymers called SMPs (shape memory polymers) can be triggered by a process in which specific chemicals diffuse into the structure causing a reversal in both shape and stiffness after deformation [9]. Similarly, SMAs (shape memory alloys) can change their stiffness when affected by changes in temperature and have been used extensively in many soft robotic tasks such as manipulation ([10], [11]).

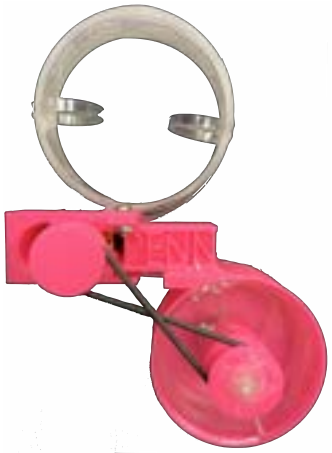

Fig. 1. Proposed Tunable Stiffness Spring Design. Consisting of a single motor, and a PET ring

On top of material science solutions to variable stiffness, there are numerous mechanical designs that leverage a variety of solutions such as friction, pressure, and topology to affect a change in stiffness. The McKibben muscle is one of the most famous pneumatic or hydraulic soft actuator. By increasing the internal pressure of a flexible tube, the mechanism can increase in diameter, and shorten in length which will alter the overall stiffness of the muscle. Another pneumatic solution involves a physics principal called jamming where a decrease in pressure of a tube that is filled with particles or thin sheets jams the internal components together and stiffens the entire structure through friction. There are also numerous motor driven solutions such as jack springs [12], leaf springs [13], SEAs (series elastic actuator), VSAs (variable stiffness actuator) [14], and more. Auxetics, which are materials with a negative Poisson's ratio, have been used in a concentric tube structure to achieve a variable stiffness system [15]. Origami has also been used in conjunction with other metamaterials to produce impressive tunable stiffness structures [16].

Most of the mechanical solutions above vary spring length to control spring stiffness. While many of the smart materials, such as SMAs take a large time to change in stiffness or may not produce a large enough change in stiffness to be impactful in a robot control scenario under high loads and speeds. What is missing in this research is a solution for a large, fast change in stiffness without affecting other spring parameters such as length.

This work outlines a design for a spring that can produce

large changes in stiffness in a short period of time, while also maintaining other spring parameters such as relaxed length or diameter. To achieve this, we propose an electromechanically tunable stiffness spring. This mechanism would consist of a thin PET sheet bent into a ring with many layers that we can add or remove continuously from the center to change the effective thickness of the ring without affecting it's outside diameter. By compressing this ring we form a spring that increases in stiffness with an increase in layers from the PET sheet. We propose a model, and validation using a multitude of practical stiffness tests while changing spring parameters such as ring diameter, material thickness and width, as well as the amount of layers in the spring.

Finally we demonstrate the capability of our spring in a tunable stiffness manipulator. By using our deformation model, we can build a variable stiffness spring segment and corresponding lyapunov stable controller as an application. This compliant structure consists of four of our variable stiffness springs, and a singular motor for global compression. This design allows for a precise 3D positioning structure that is modular and could be stacked to produce non-constant curvature shapes, as well as force control which wouldn't be possible without a spring with these properties.

II. Theoretical Model

Our main goal in this section is to describe how we modeled the deformation of the spooled material inside our spring.

A. Assumptions

To simplify this problem, we assume that this spool is a set of nested concentric elastic rings where the inside diameter of one ring touches the outside diameter of the ring inside of it. We also make the assumption that each ring is compressed between two plates that are always flat. This allows us to model each ring separately which will greatly simplify our mathematical model. Extending on the flat plate compression assumption, we will assume that our deformations are vertically symmetric.

In this paper we also look at states where the material inside the spool doesn't make a full circle, leaving us with a half-ring. For this, we assume the amount of material in an unfinished ring maps linearly to the amount of force a full ring of the same diameter would produce.

B. Nomenclature

Using the model proposed in [17] to model the compression of concentric elastic rings we can introduce the following parameters listed in Table I & Table II.

TABLE I
Ring Parameters

D	Diameter of the ring measured from the centerline of the material
H	Thickness of the ring material
W	Width of the ring material
L	Circumference of the ring
S	Arc length of the ring
E	Elastic modulus of the ring
$I\ (=\frac{WH^3}{12})$	Cross-sectional moment of inertia of the ring
B	Contact length between the ring and the plate.
F	Downward load on the ring

The most notable parameter from this table is S. The arc length of the ring. Our model utilizes a non-dimensional differential equations with a derivative of S. To supplement this, Table II lists the functions of S that are important to our problem.

TABLE II
Functions of S

$\theta(S)$	Tangent angle of the ring measured from the horizontal
$X(S)$	Horizontal coordinate of the ring
$Y(S)$	Vertical coordinate of the ring
$M(S)$	Internal bending moment
$P(S)$	Internal horizontal force
$Q(S)$	Internal vertical force

C. Single Ring Compression Model

Due to the geometry of how rings compress, there are two states that need to be modeled separately. During the initial portion of compression, the plate only contacts the ring at the very top and bottom of the circle. This behaviour is shown in the first model in Figure 4. There is a force threshold where the ring contacts the top and bottom plates at more than just a single point. At this compression point, we swap to a second model that takes this into account which is shown in Figure 5. The variable that represents the length contact between the ring and the plate is B. Because of the assumption that our ring deformations are vertically symmetric, we will only model the right side of the ring starting when it first stops contact with the bottom plate. This means that as we compress, the origin of our model will change depending on how much of the ring is contacting the base plate. This can be seen in the illustration in Figure 2 & Figure 3 where the origin moves to the liftoff point as the ring is compressed. The non-dimensional variables that are constructed for our model are shown in Equation 1.

$$\begin{gathered} x=\frac{X}{L},\ y=\frac{Y}{L},\ s=\frac{S}{L},\ b=\frac{B}{L}, \\ f=\frac{FL^2}{EI},\ p=\frac{PL^2}{EI},\ q=\frac{QL^2}{EI},\ m=\frac{ML}{EI} \end{gathered} \tag{1}$$

The non-dimensional governing equations that utilize these variables to model our ring system are listed in Equation 2

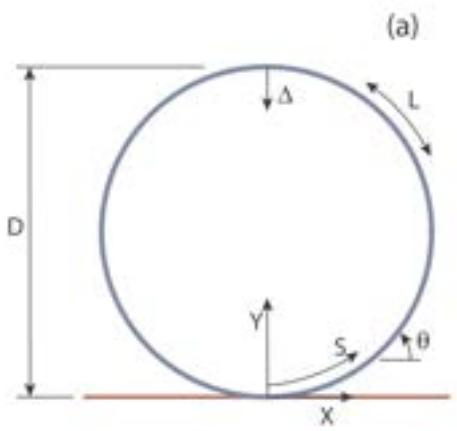

Fig. 2. Ring parameter diagram for point load forces

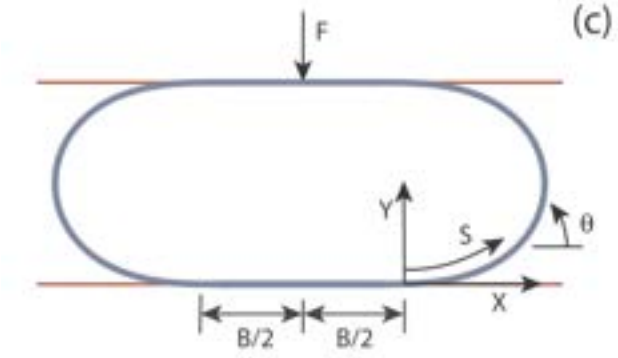

Fig. 3. Ring parameter diagram for plate load forces

and are pulled from references [17], [18], & [19].

$$\frac{\partial x}{\partial s} = \cos\theta,\ \frac{\partial y}{\partial s} = \sin\theta,$$
$$\frac{\partial \theta}{\partial s} = m + 2\pi,\ \frac{\partial m}{\partial s} = \frac{f}{2}\cos\theta - p\sin\theta \qquad (2)$$

Using these equations, we can solve for the ring compression from a given f for both states of compression- the point load model, and the plate load model. To solve for these, we used MATLAB $ode45$ and $fsolve$ to construct, and solve this second-order equation similar to using a shooting method. To do this, a set of initial and final conditions must be given for your variables in order to achieve the desired state. We also must specify what to integrate over, which in this case is s.

1) Solving Point Load Compressions: Since we have nondimensionalized our variables, this model has an arc length of 1 from the bottom to the top of the right half of the circle. From Figure 2 we can see that our integration origin point is at the very bottom of the circle for the point load. So, our range for s is just 0-1. With that in mind, and a user-chosen compression force f, we can feed in the following conditions to solve our equation:

Initial conditions: $x = 0,\ y = 0,\ \theta = 0,\ m = ?,\ p = ?$

Final conditions: $x = 0,\ \ \theta = \pi$

The values with question marks are the variables that we use $fsolve$ to optimize so our $ode45$ solution fits the desired final parameters after integration. Now that we have a working model for a specific force, we can vary f and generate a force-displacement plot for this model for any force value before plate load compression occurs. This can be seen in Figure 4

2) Solving Plate Load Compressions: The plate load model is very similar to the point load model. We can reuse the same equations, however initial conditions, and the parameters we vary to fit our final parameters change. The largest change is the amount we integrate over in s. Since we start our origin at the liftoff point of the ring, and a portion of our ring is flat against the plate we can no longer assume an s from 0-1. We must subtract the amount of material that is flat against the plates on the top and the bottom to get a correct integration length. So the maximum value of s should be $\frac{1-2b}{2}$ where b represents the non-dimensional contact length between the ring and the plate. So our new s range is 0 to $\frac{1-2b}{2}$. It should be noted that one of the new parameters that we optimize for in this model compared to the point model is b. So, the integration length isn't known until the equation is fully solved. Below is the list of conditions for this plate model based on an initial input for f:

Initial conditions: $x = 0,\ y = 0,\ \theta = 0,\ m = -2\pi,$
$p = ?,\ b = ?$ (3)

Final conditions: $x = 0,\ \ \theta = \pi$

We can now generate force values for the compression force for this model, and combine it with the plate model to produce a continuous force-deformation plot. These results can be seen in Figure 5

D. Nested Ring Compression Model

Now that we have a continuous compression model for a singular ring, we can extend this to our problem- sets of nested rings. Utilizing our assumption that the outside diameter of one ring touches the inside diameter of the ring larger than it, we can model our set of rings as each having the same amount of compression. Because, as soon as you compress the outer ring, all the rings inside of it must also compress that same amount due to no gaps in between ring layers. So our final force-compression curve is a dimensionalized sum of each of the force-compression curves of the ring layers inside the coil. This is the model that we will use to compare to our experimental results, and employ in our tunable stiffness manipulator.

III. Tunable Stiffness Spring

A. Design

Our spring in Figure 6 consists of a ring that is made using 10mil PET (Polyethylene terephthalate) film. This outside

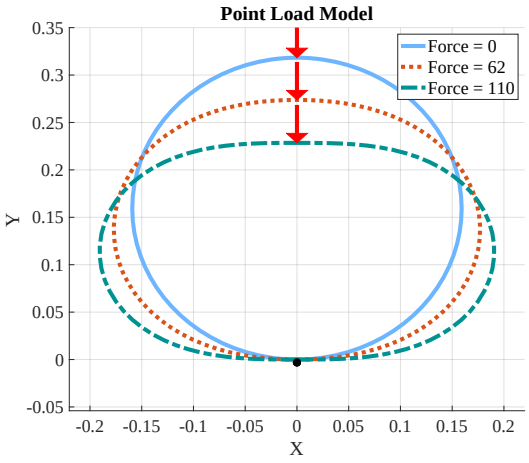

Fig. 4. This figure shows how a non-dimensional ring deforms with a force from a range of 0 - 110.

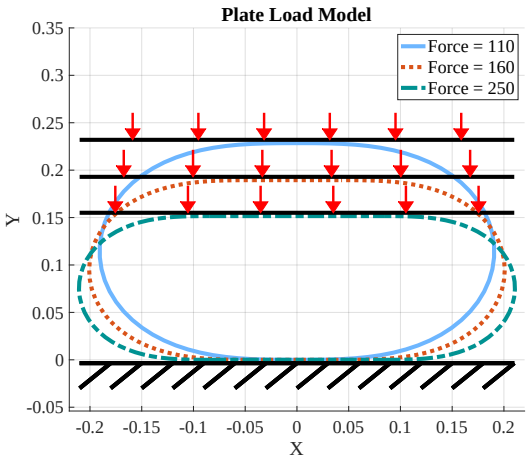

Fig. 5. This figure shows how a non-dimensional ring deforms with a force from a range of 110 - 250.

ring dictates the outside diameter of the spring. Inside this ring lies 7mil PET of the shelf balloon tape which is 15mm wide film with .25" holes every .5". This balloon tape can be spooled inside the spring, effectively increasing the thickness of the ring which increases its stiffness. We can control the amount of spooled material with a micro motor attached to a gear which can interface with the holes in the balloon tape to move material inside the spring, or out of the spring into a storage container. This storage container actively spools the material inside an enclosed space to keep the material ready to use inside the spring. This container is powered with a twisted o-ring belt system from the main micro motor that actuates the balloon tape material. This allows us to utilize only one motor for our design, which reduces overall weight.

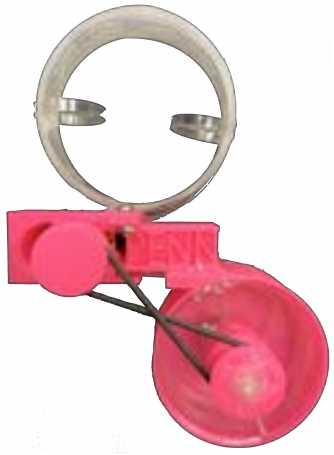

Fig. 6. Tunable stiffness spring. Printed in PLA using a Prusa Mini at 15% infill.

IV. Experiments

A. Single Spring Experiments

Using an MTS (Material Test System) machine, we constructed springs of varying widths, diameters, and material thicknesses in order to analyze our model fit to experimental data. This system generates Force-displacement data that we can directly match with our model after we dimensionalize our solution with the specific ring constants. For each spring, we gathered a force-displacement curve for a set of 1-20 coils at half-coil intervals. An example of this data is shown in Figure 7.

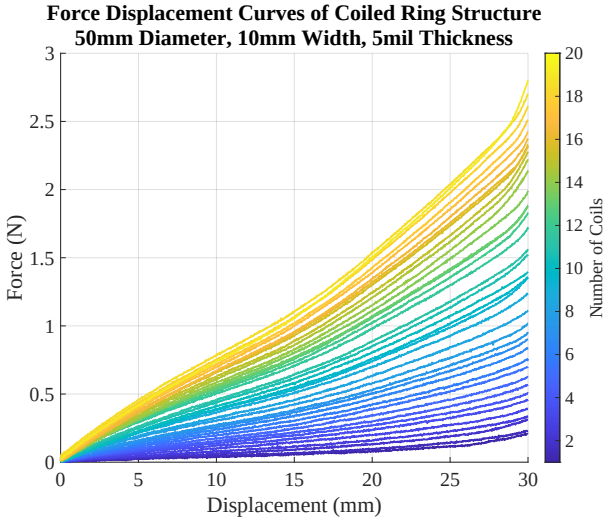

Fig. 7. Experimental MTS test for a range of 1-20 coils with a total compression amount of 30mm.

We performed identical tests to the ones in Figure 7 with different springs with slightly different material thicknesses, diameters, and widths and then compared the results to our theoretical model. The resulting percent error scaled by maximum force in the test is shown in Figure 8

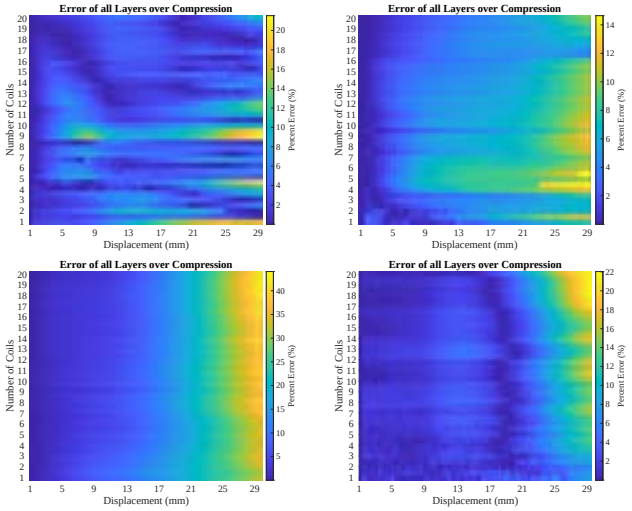

Fig. 8. Four tests with various springs compared to theoretical model. Each test has a separate percent error scale due to the changes in maximum force for the experiments. It can be seen that with less compression, our model fits much better than with large deformations. We believe this is due to friction, material plastic deformation, gaps between the coils, and model assumptions.

B. Manipulator Experiments

Using this spring, we built a 4DOF manipulator shown in Figure 9. This manipulator utilizes four tunable stiffness springs in a square shape connected with a plate on the top and the bottom, connected with an actuated string. When the string is pulled, the system will compress, and will return to it's original state when the string is released. Using this system we can control the angle and height of the top plate, as well as the stiffness of the total structure.

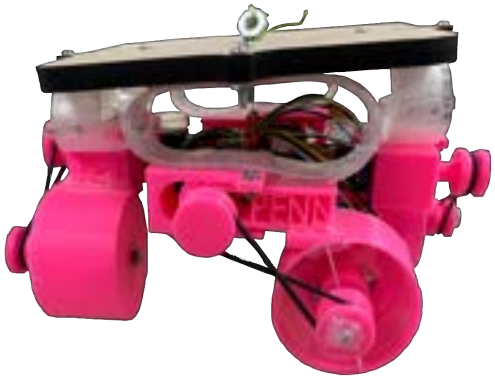

Fig. 9. Spring Module

1) Workspace Experiments: Using this system, we performed some manipulator workspace experiments by placing the springs at extreme opposites of stiffnesses, and compressing the module fully. By replicating this process for all four sides, and then at the corners of the square we can construct an approximated manipulator workspace that is shown in Figure 10

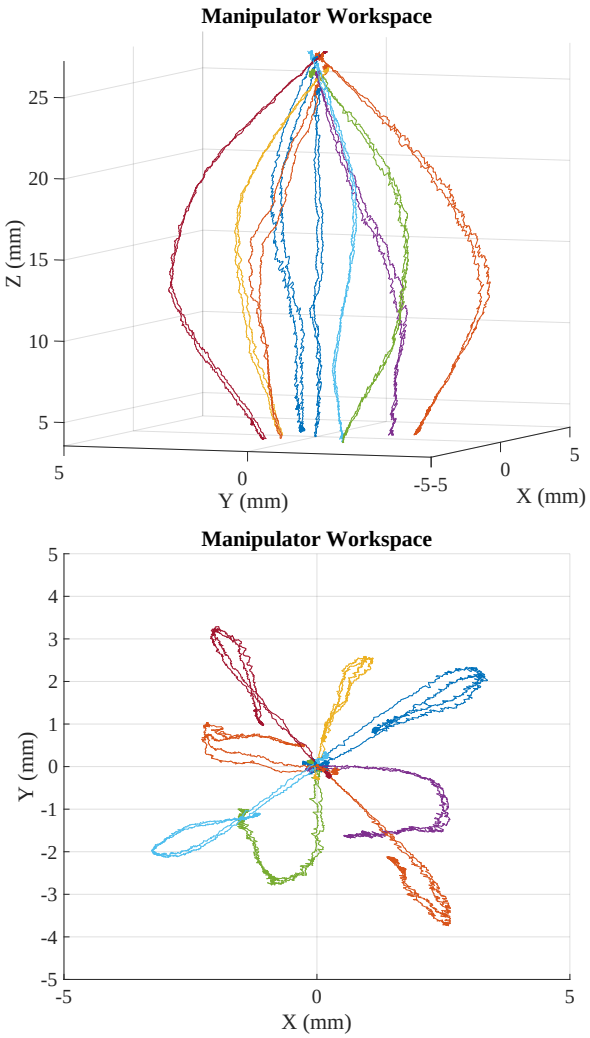

Fig. 10. Culmination of workspace tests for the tunable stiffness manipulator. Data was gathered by tracking the position of the top plate of the structure using a motion capture system.

Once we have attained the workspace, we can begin pathing positions for our manipulator to follow. Figure 11 shows our attempts at creating a square, and a circle respectively.

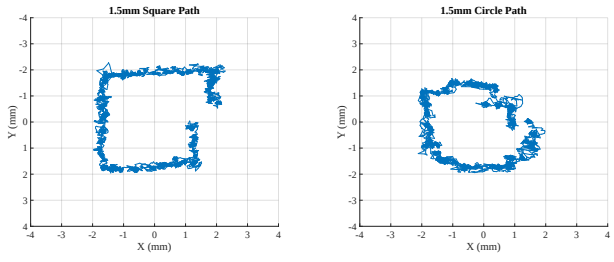

Fig. 11. Pathing tests for a 1.5mm Square, and 1.5mm Circle. These tests took place over approximately 1.5 minutes.

V. Conclusion

In this paper we introduced a model and design for a novel tunable stiffness spring design that is fast, lightweight, and can be utilized for millimeter accurate use in complex soft mechanisms. This work more broadly is intended to introduce the concept of coiled film as a strategy to attain simple tunable stiffness structures. Our methods are purposely easily replicatable with a 3D printer and off the shelf motors and plastic materials.

References

[1] Guanjun Bao, Hui Fang, Lingfeng Chen, Yuehua Wan, Fang Xu, Qinghua Yang, and Libin Zhang.Soft Robotics.Jun 2018.229-241.http://doi.org/10.1089/soro.2017.0135

[2] Lee, C., Kim, M., Kim, Y.J. et al. Soft robot review. Int. J. Control Autom. Syst. 15, 3–15 (2017). https://doi.org/10.1007/s12555-016-0462-3

[3] Polygerinos, Panagiotis et al. "Soft Robotics: Review of Fluid-Driven Intrinsically Soft Devices; Manufacturing, Sensing, Control, and Applications in Human-Robot Interaction." Advanced engineering materials. 19.12 (2017): n. pag. Web.

[4] Zhang, Yongchang, et al. "Progress, Challenges, and Prospects of Soft Robotics for Space Applications." Advanced Intelligent Systems., 2022, p. 2200071., https://doi.org/10.1002/aisy.202200071.

[5] Mark Runciman, Ara Darzi, and George P. Mylonas.Soft Robotics.Aug 2019.423-443.http://doi.org/10.1089/soro.2018.0136

[6] R. V. Ham, T. G. Sugar, B. Vanderborght, K. W. Hollander and D. Lefeber, "Compliant actuator designs," in IEEE Robotics & Automation Magazine, vol. 16, no. 3, pp. 81-94, September 2009, doi: 10.1109/MRA.2009.933629.

[7] Morishita, S., and Mitsui, J. (July 1, 1992). "Controllable Squeeze Film Damper (An Application of Electro-Rheological Fluid)." ASME. J. Vib. Acoust. July 1992; 114(3): 354–357.

[8] G. Rizzello, D. Naso, A. York and S. Seelecke, "Modeling, Identification, and Control of a Dielectric Electro-Active Polymer Positioning System," in IEEE Transactions on Control Systems Technology, vol. 23, no. 2, pp. 632-643, March 2015, doi: 10.1109/TCST.2014.2338356.

[9] Dumlu H, Marquardt A, Zirdehi EM, Varnik F, Shen Y, Neuking K, Eggeler G. A Mechanical Analysis of Chemically Stimulated Linear Shape Memory Polymer Actuation. Materials (Basel). 2021 Jan 20;14(3):481.

[10] Liang C, Rogers CA. Design of Shape Memory Alloy Springs with Applications in Vibration Control. Journal of Intelligent Material Systems and Structures. 1997;8(4):314-322.

[11] Junfeng Li, Position control based on the estimated bending force in a soft robot with tunable stiffness, Mechanical Systems and Signal Processing, Volume 134, 2019, 106335, ISSN 0888-3270,

[12] K. W. Hollander, T. G. Sugar and D. E. Herring, "Adjustable robotic tendon using a 'Jack Spring'", Proc. Int. Conf. Rehabil. Robot., pp. 113-118, 2005.

[13] J. Choi, S. Hong, W. Lee, S. Kang and M. Kim, "A Robot Joint With Variable Stiffness Using Leaf Springs," in IEEE Transactions on Robotics, vol. 27, no. 2, pp. 229-238, April 2011

[14] G. Tonietti, R. Schiavi and A. Bicchi, "Design and Control of a Variable Stiffness Actuator for Safe and Fast Physical Human/Robot Interaction," Proceedings of the 2005 IEEE International Conference on Robotics and Automation, 2005, pp. 526-531, doi: 10.1109/ROBOT.2005.1570172.

[15] Xiang Yu Zhang, Xin Ren, Xin Yuan Wang, Yi Zhang, Yi Min Xie, A novel combined auxetic tubular structure with enhanced tunable stiffness, Composites Part B: Engineering, Volume 226, 2021, 109303, ISSN 1359-8368, https://doi.org/10.1016/j.compositesb.2021.109303.

[16] Zhai Z., Wang Y., Jiang H. Origami-inspired, on-demand deployable and collapsible mechanical metamaterials with tunable stiffness Proc. Natl. Acad. Sci., 115 (9) (2018), pp. 2032-2037

[17] R. H. Plaut and L. N. Virgin, "Deformation and vibration of upright loops on a foundation and of hanging loops," International Journal of Solids and Structures, vol. 51, no. 18, pp. 3067–3075, 2014. [Online]. Available: https://www.sciencedirect.com/science/article/pii/S0020768314001899

[18] R. Plaut, J. Sidbury, and L. Virgin, "Analysis of buckled and pre-bent fixed-end columns used as vibration isolators," Journal of Sound and Vibration, vol. 283, no. 3, pp. 1216–1228, 2005. [Online]. Available: https://www.sciencedirect.com/science/article/pii/S0022460X04006431

[19] R. H. Plaut and L. N. Virgin, "Deformation and vibration of upright loops on a foundation and of hanging loops," International Journal of Solids and Structures, vol. 51, no. 18, pp. 3067–3075, 2014. [Online]. Available: https://www.sciencedirect.com/science/article/pii/S002076831400189